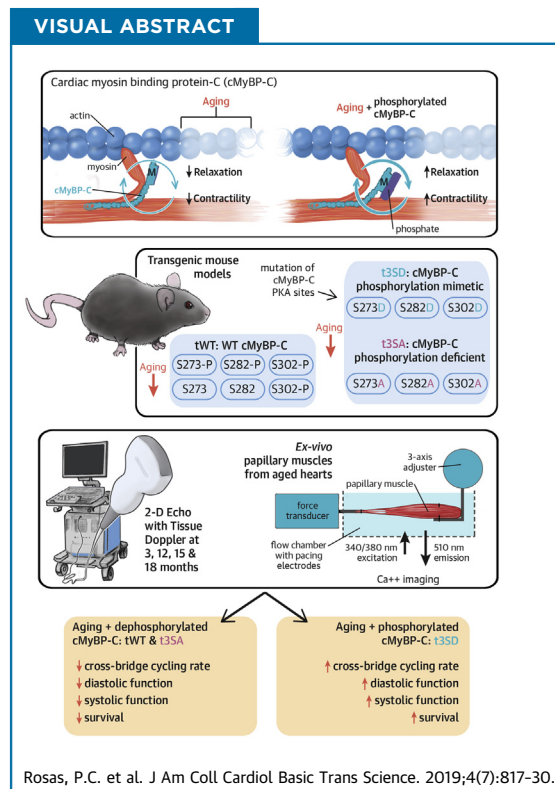**PRECLINICAL RESEARCH**

Cardiac Myosin Binding Protein-C Phosphorylation Mitigates Age-Related Cardiac Dysfunction

Hope for Better Aging?

Paola C. Rosas, MD, PhD, BSPharm,[a] Chad M. Warren, MS,[a] Heidi A. Creed, BS,[b] Jerome P. Trzeciakowski, PhD,[b]
R. John Solaro, PhD,[a] Carl W. Tong, MD, PhD[b,c]

VISUAL ABSTRACT

Rosas, P.C. et al. J Am Coll Cardiol Basic Trans Science. 2019;4(7):817–30.

HIGHLIGHTS

- With aging, phosphorylated-mimetic cMyBP-C mice exhibited better survival, better preservation of systolic and diastolic functions, and unchanging wall thickness compared with control mice.
- Aged wild-type equivalent mice exhibited decreasing cMyBP-C phosphorylation (S273 and S282) along with worsening cardiac function and hypertrophy similarly to what was observed in hypophosphorylated cMyBP-C mice.
- Intact papillary muscle experiments suggest that cMyBP-C phosphorylation increased cross-bridge detachment rates as the underlying mechanism.
- Phosphorylating cMyBP-C is therefore a novel mechanism that can prevent aging-related development of cardiac dysfunction.

ABBREVIATIONS AND ACRONYMS

3SA = mutated 3 serines to 3 alanines to mimic hypophosphorylated cardiac myosin binding protein-C (S273A, S282A, and S302A)

3SD = mutated 3 serines to 3 aspartic acids to mimic phosphorylated cMyBP-C (S273D, S282D, and S302D)

ANOVA = analysis of variance

cMyBP-C = cardiac myosin binding protein-C

cTnI = cardiac troponin I

EF = ejection fraction

HF = heart failure

HFpEF = heart failure with preserved ejection fraction

HOP = hydroxyproline

LV = left ventricular

SUMMARY

Cardiac myosin binding protein-C (cMyBP-C) phosphorylation prevents aging-related cardiac dysfunction. We tested this hypothesis by aging genetic mouse models of hypophosphorylated cMyBP-C, wild-type equivalent, and phosphorylated-mimetic cMyBP-C for 18 to 20 months. Phosphorylated-mimetic cMyBP-C mice exhibited better survival, better preservation of systolic and diastolic functions, and unchanging wall thickness. Wild-type equivalent mice showed decreasing cMyBP-C phosphorylation along with worsening cardiac function and hypertrophy approaching those found in hypophosphorylated cMyBP-C mice. Intact papillary muscle experiments suggested that cMyBP-C phosphorylation increased cross-bridge detachment rates as the underlying mechanism. Thus, phosphorylating cMyBP-C is a novel mechanism with potential to treat aging-related cardiac dysfunction. (J Am Coll Cardiol Basic Trans Science 2019;4:817–30) © 2019 The Authors. Published by Elsevier on behalf of the American College of Cardiology Foundation. This is an open access article under the CC BY-NC-ND license (http://creativecommons.org/licenses/by-nc-nd/4.0/).

Heart failure (HF) afflicts 6.2 million Americans as of 2019 [1]. The prevalence of HF is expected to increase to >8 million by 2030 [2]. HF prevalence also increases with age, from 0.3% (male) and 0.2% (female) of the population at ages 20 to 39 years to 6.9% (male) and 4.8% (female) at ages 60 to 79 years according to the National Health and Nutrition Examination Survey (2013 to 2016). Aging alone can lead to deterioration of diastolic function, despite improvement in blood pressure control [3]. Moreover, HF is the leading cause of hospitalization in elderly patients [4]. Despite new treatments, ~50% of patients diagnosed with HF will die within 5 years [1]. Therefore, we need to search for novel strategies to treat this deadly disease in our aging population.

Cardiac myosin binding protein-C (cMyBP-C), a heart muscle thick filament protein, can regulate cross-bridge attachment/detachment processes by its phosphorylation status. Once phosphorylated, cMyBP-C accelerates cross-bridge cycling to enhance the ability of the heart to contract and relax [5,6]. Hearts from patients with hypertension [7], atrial fibrillation [8], hypertrophic cardiomyopathy [9-11], and HF [9,11,12] all exhibit decreased cMyBP-C phosphorylation levels. Moreover, cMyBP-C mutations are a predominant cause of hypertrophic cardiomyopathy that progresses to HF [13]. Thus, there is sufficient evidence to suggest that cMyBP-C phosphorylation mediates normal heart physiology.

We hypothesized that cMyBP-C phosphorylation mitigates aging-related cardiac dysfunction. To test this idea, we used existing mouse models of cMyBP-C phosphorylation mimetic cMyBP-C(t3SD) mutant, cMyBP-C dephosphorylated mimetic cMyBP-C(t3SA) mutant, and cMyBP-C wild-type cMyBP-C(tWT). These mice were aged to >18 months to mimic a 60- to 70-year-old human. Our studies found that cMyBP-C phosphorylation preserves heart function during aging.

METHODS

MOUSE LINES. All protocols for animal care and use were approved by the Institutional Animal Care and Use Committee at the Texas A and M University Health Science Center College of Medicine Temple and College Station campuses. Three mice models were used that were previously generated by transgenic expression of cMyBP-C phosphorylation mimetics on a cMyBP-C$^{(-/-)}$ null background that was

generated on an E129X1 (SVE-129) strain [14]. Three cMyBP-C protein kinase-A sites (S273, S282, and S302) were mutated to nonphosphorylatable alanine to mimic phosphorylation deficiency, cMyBP-C(t3SA) [15], or else substituted to nonphosphorylatable aspartic acid to mimic the negative charge of the phosphorylated residue, cMyBP-C(t3SD) [6]. The cMyBP-C(tWT) control was generated by re-introducing wild-type cMyBP-C into the cMyBP-C$^{(-/-)}$ null background [15]. Because the phosphorylation status of cMyBP-C can change with various conditions, we used cMyBP-C(t3SD), which mimics constitutively phosphorylated cMyBP-C, to test our hypothesis. The 3 models exhibited similar cMyBP-C expression levels: cMyBP-C(tWT): 72%; cMyBP-C(t3SA): 74%; and cMyBP-C(t3SD): 84% [6,15].

SURVIVAL. The mice models were aged to >18 months to mimic 60- to 70-year-old human subjects. Both male and female mice were used. Mice euthanized for experiments or for noncardiac reasons (e.g., dermatitis, teeth problems, penile prolapse) were censored at the date of event. Survival analyses were done on day 600. Mice living beyond 600 days were censored at day 600. Censored mice were not counted as death.

MEASUREMENT OF PHYSIOLOGICAL PARAMETERS. Blood glucose and systolic blood pressure levels (tail cuff measurements on restrained conscious mice) were measured in all 3 mice models at 15 to 18 months of age. Mice were euthanized and organs were harvested to measure lung weight/body weight, heart weight/body weight, and heart weight/tibia length ratios as indicators of pulmonary edema and cardiac hypertrophy.
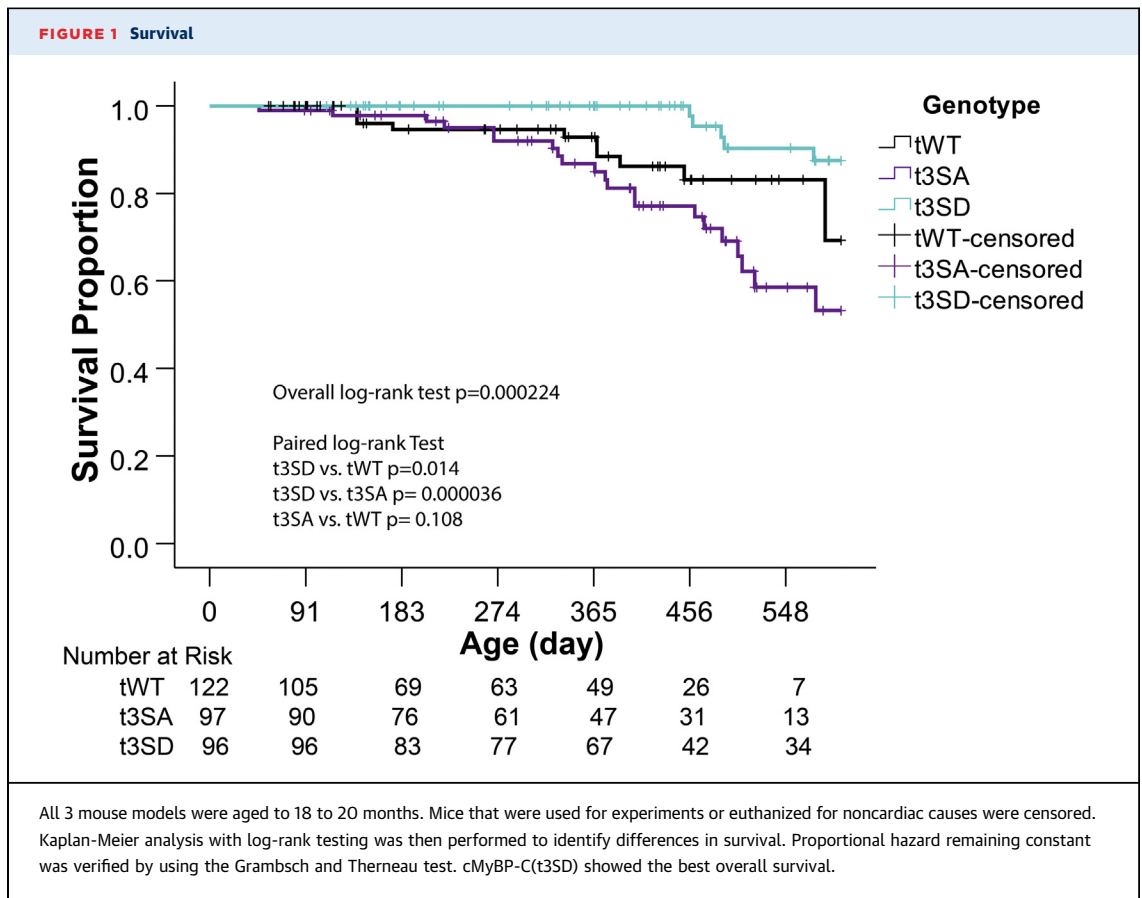
ECHOCARDIOGRAPHY. The Vevo 2100 system (FUJIFILM VisualSonics, Toronto, Ontario, Canada) was used to perform echocardiography on mice 3 to 18 months old by using a previously developed protocol [6]. Mice were anesthetized with 0.5% to 2.5% of isoflurane and placed in a warmed echocardiogram table at 39°C. Electrocardiogram, heart rate, and respiration rates were continuously monitored. The isoflurane concentration was adjusted to keep the heart rate at 380 to 450 beats/min. We performed transthoracic 2-dimensional, M-mode, color-flow Doppler, and tissue Doppler imaging. All mice completely recovered after the echocardiography studies.

FORCE AND CALCIUM MEASUREMENTS ON INTACT PAPILLARY MUSCLES. Intact papillary muscles were isolated from 12- to 15-month-old mice models. We performed simultaneous intracellular calcium $[Ca^{2+}]_i$ and force measurements using a previously developed protocol [6,16]. Briefly, right ventricular papillary muscles were isolated, mounted in a chamber, and superfused with Krebs-Henseleit solution (NaCl 119 mmol/l, glucose 12 mmol/l, KCl 4.6 mmol/l, NaHCO$_3$ 25 mmol/l, KH$_2$PO$_4$ 1.2 mmol/l, MgCl$_2$ 1.2 mmol/l, and CaCl$_2$ 1.8 mmol/l) at room temperature. Muscles were stretched to achieve maximum twitch force while maintaining steady diastolic force and paced at 1, 1.5, and 2 Hz to mimic increasing heart rate. Force was measured by using a force transducer (Aurora Scientific, Aurora, Ontario, Canada), and intracellular calcium $[Ca^{2+}]_i$ was estimated by using Fura-2 as an indicator along with a hyperswitch system (IonOptix LLC, Westwood, Massachusetts). Fluorescence was recorded at 510 nm from calcium-bound Fura-2 (340 nm excitation) and calcium-free Fura-2 (380 nm of excitation). We calculated $[Ca^{2+}]_i$ using calcium-bound Fura-2/calcium-free Fura-2 ratios after background correction [6].

MYOFIBRILLAR PREPARATIONS. Snap-frozen left ventricular (LV) tissue was homogenized twice by using glass Dounce homogenizers in standard relax buffer (imidazole 10 mM, pH 7.2, KCl 75 mM, MgCl$_2$ 2 mM, ethylenediaminetetraacetic acid 2 mM , and NaN$_3$ 1 mM) with 1% (v/v) Triton X-100, as previously described [17]. Myofibrils were centrifuged, and the supernatant fraction was removed. The pellets were then washed once in standard relax buffer to remove the Triton X-100. The standard relax buffers contained both the protease (MilliporeSigma, St. Louis, Missouri) and phosphatase (Calbiochem, Darmstadt, Germany) inhibitors at a 1:100 dilution and Calyculin A (Cell Signaling Technology, Danvers, Massachusetts) to 100 nM final concentration. The pellet was solubilized in the sample buffer containing urea 8 M, thiourea 2 M, Tris 0.05 M, dithiothreitol 75 mM , and sodium dodecyl sulfate 3% . Protein concentration of the samples was determined with a Pierce 660 nm protein assay reagent with the addition of an ionic detergent compatibility reagent (Thermo Fisher Scientific, Waltham, Massachusetts). Samples were stored at -80°C until used.

PROTEIN PHOSPHORYLATION. Myofibrillar preparations were analyzed with a 12% sodium dodecyl sulfate-polyacrylamide gel electrophoresis method. Pro-Q Diamond phosphoprotein staining (Thermo Fisher Scientific) was used to estimate the amount of phosphorylated proteins, and Coomassie staining was used to estimate the amount of loaded proteins as previously described [6]. The gel was imaged on a ChemiDoc MP (Bio-Rad, Hercules, California), and band densities were determined by using Image Lab 6.0.1 software.
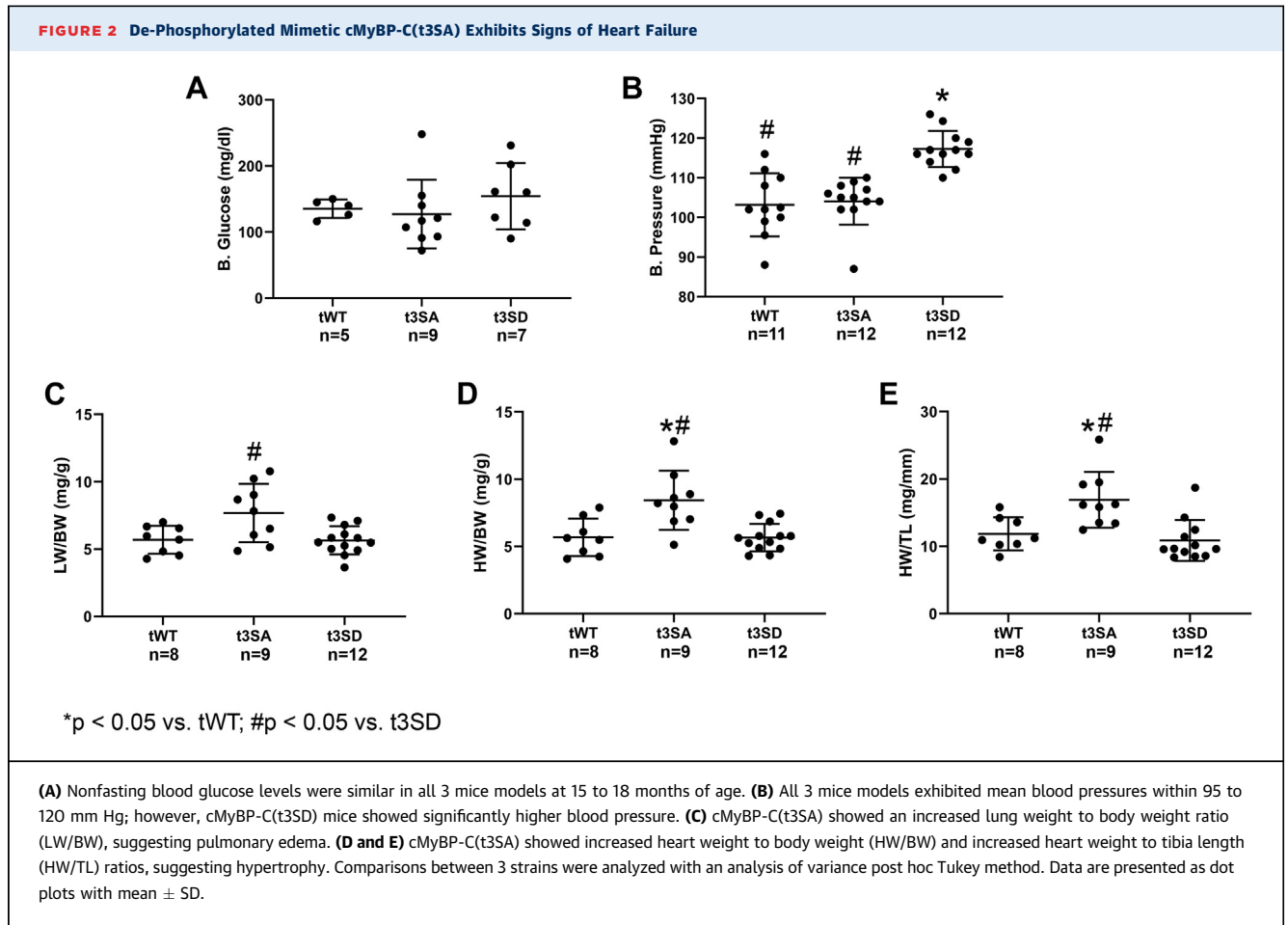
FIGURE 1 Survival

Overall log-rank test p=0.000224

Paired log-rank Test
t3SD vs. tWT p=0.014
t3SD vs. t3SA p= 0.000036
t3SA vs. tWT p= 0.108

Number at Risk	0	91	183	274	365	456	548
tWT	122	105	69	63	49	26	7
t3SA	97	90	76	61	47	31	13
t3SD	96	96	83	77	67	42	34

All 3 mouse models were aged to 18 to 20 months. Mice that were used for experiments or euthanized for noncardiac causes were censored. Kaplan-Meier analysis with log-rank testing was then performed to identify differences in survival. Proportional hazard remaining constant was verified by using the Grambsch and Therneau test. cMyBP-C(t3SD) showed the best overall survival.

WESTERN BLOTTING WITH FLUORESCENT DETECTION. After gel electrophoresis, proteins were transferred to a 0.22 μm WesternBright PVDF-FL membrane (Advansta, San Jose, California). Blots were blocked for 1 h with AdvanBlock Fluor (Advansta) and then probed in primary antibodies diluted in AdvanBlock Fluor overnight at 4°C. The phospho-specific (S273P, S282P, and S302P) cMyBP-C antibodies were generous gifts from Sakthivel Sadayappan, PhD (University of Cincinnati College of Medicine, Cincinnati, Ohio), and the total mouse monoclonal cMyBP-C antibody was from Santa Cruz Biotechnology (Dallas, Texas) (#SC-137181) and was diluted to 1:2,500. The membranes were washed and then incubated with secondary antibodies diluted in AdvanBlock Fluor. We used secondary goat anti-rabbit DyLight 800 4X PEG (#SA5-35571, Thermo Fisher Scientific) 1:10,000 and secondary goat anti mouse StarBright Blue 700 (#12004158, Bio-Rad) 1:5,000. Membranes were imaged on a ChemiDoc MP (Bio-Rad), and band densities were determined by using Image Lab 6.0.1 software.

HYDROXYPROLINE ASSAY. Hydroxyproline (HOP) content was determined as previously described (18). A portion of the LV posterior wall (i.e., LV free wall) was removed in a similar region for all hearts. This region corresponded to echocardiographic measurements of posterior wall thickness. To determine the exact weight of the tissue, 15 to 25 mg of snap-frozen cardiac tissue was minced into a screw cap vial. Tissue was covered with 6 M of hydrochloric acid and incubated in an oven at 105°C to 110°C overnight. We used a standard curve of *trans*-4-Hydroxy-L-proline (H-55409, MilliporeSigma) (0 to 500 μM) to determine the content of HOP per milligram of tissue.

STATISTICAL ANALYSES. SPSS version 25 (IBM SPSS Statistics, IBM Corporation, Armonk, New York) and Stata version 14 (StataCorp, College Station, Texas) software were used to complete statistical analyses. Kaplan-Meier curves and log-rank tests were used to identify significant differences in survival. Analysis of variance (ANOVA) was used to identify significant differences among 3 groups with a post hoc Tukey

FIGURE 2 De-Phosphorylated Mimetic cMyBP-C(t3SA) Exhibits Signs of Heart Failure

*p < 0.05 vs. tWT; #p < 0.05 vs. t3SD

(A) Nonfasting blood glucose levels were similar in all 3 mice models at 15 to 18 months of age. **(B)** All 3 mice models exhibited mean blood pressures within 95 to 120 mm Hg; however, cMyBP-C(t3SD) mice showed significantly higher blood pressure. **(C)** cMyBP-C(t3SA) showed an increased lung weight to body weight ratio (LW/BW), suggesting pulmonary edema. **(D and E)** cMyBP-C(t3SA) showed increased heart weight to body weight (HW/BW) and increased heart weight to tibia length (HW/TL) ratios, suggesting hypertrophy. Comparisons between 3 strains were analyzed with an analysis of variance post hoc Tukey method. Data are presented as dot plots with mean ± SD.

alpha-correction method to adjust for multiple pairwise comparisons. Student's *t*-test was used to compare 2 independent groups. Repeated measure ANOVA with intergroup comparison was used to identify significant differences in responses to increasing pacing frequency on intact papillary muscles among the 3 mouse models. Pearson correlation was used to test for a linear correlation between 2 continuous variables. When possible, dot plots with mean ± SD were used to present data. Statistical significance was determined by using a 2-sided p value <0.05.

RESULTS

cMyBP-C PHOSPHORYLATION MIMETIC cMyBP-C(t3SD) MICE EXHIBITED BETTER SURVIVAL. Kaplan-Meier analysis showed significantly different survival at 600 days in all 3 mice models (overall log-rank test, p < 0.001). Results are as follows: cMyBP-C(tWT) at 69.3 ± 0.1% survival, starting n = 122 (112 censored; 5 censored for age >600 days); cMyBP-C(t3SA) at

53.2 ± 0.1% survival, starting n = 97 (76 censored; 10 censored for age >600 days); and cMyBP-C(t3SD) at 87.5 ± 0.1% survival, starting n = 96 (91 censored; 22 censored for age >600 days). Pairwise comparison log-rank testing revealed that cMyBP-C(t3SD) exhibited significantly better survival than the other 2 mouse models, and cMyBP-C(tWT) trended toward better survival than cMyBP-C(t3SA) (**Figure 1**).

cMyBP-C(t3SA) HYPOPHOSPHORYLATED MIMETIC AGED MICE SHOWED SIGNS OF HEART FAILURE NOT ATTRIBUTABLE TO DIABETES OR HYPERTENSION.
Nonfasting blood glucose measurements were similar between mice models age 15 to 18 months (**Figure 2A**). Tail cuffs were used to measure systolic blood pressure at 15 to 18 months of age. All 3 models exhibited blood pressure levels within normal ranges (mean systolic blood pressure <120 mm Hg) (19); however, cMyBP-C(t3SD) showed significantly higher blood pressures than the other 2 groups (**Figure 2B**). cMyBP-C(t3SA) mice exhibited an increased lung/body weight ratio, indicating pulmonary edema (**Figure 2C**). cMyBP-C(t3SA) mice showed increased heart weight/

FIGURE 3   **cMyBP-C Phosphorylated Mimetic (t3SD) Demonstrated Better Preservation of Diastolic and Systolic Functions With Aging**
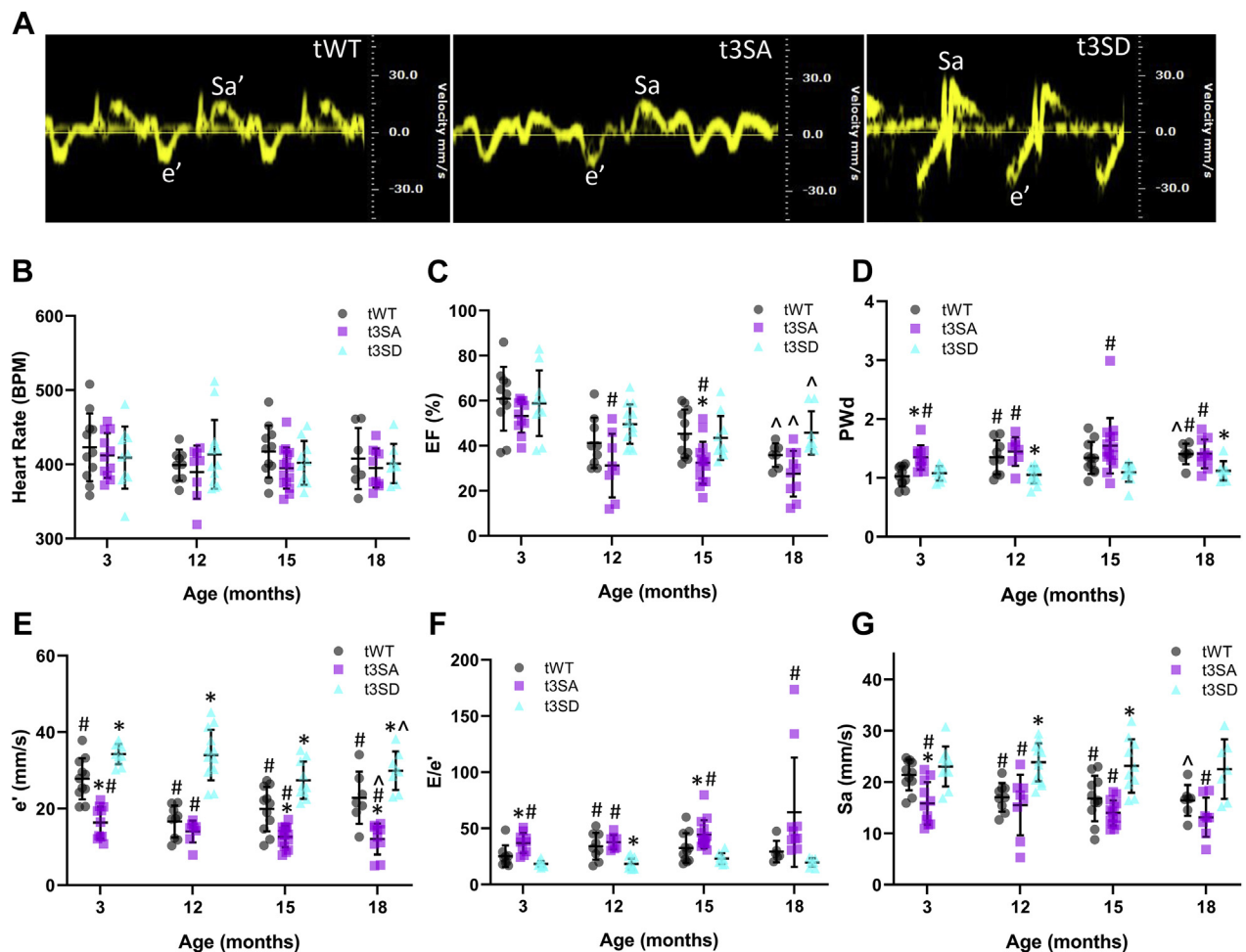
(A) Sample tissue Doppler traces showed that cMyBP-C(t3SD) myocardium relaxes at a much faster velocity (e′) during early diastole at 15 months of age. (B) All mice models showed similar heart rates. (C) cMyBP-C(t3SD) showed better preservation of ejection fraction (EF). (D) Only cMyBP-C(t3SD) showed preserved posterior wall thickness during diastole (PWd) with aging. (E) cMyBP-C(t3SD) exhibited faster peak myocardial relaxation velocity (e′) that was preserved with aging. (F) cMyBP-C(t3SD) showed preservation of E/e′ with aging. (G) Peak myocardial contraction velocity (Sa) was preserved in cMyBP-C(t3SD) hearts. cMyBP-C(tWT), 3 months: n = 11; 12 months: n = 9; 15 months: n = 11; and 18 months: n = 7. cMyBP-C(t3SA), 3 months: n = 11; 12 months: n = 8; 15 months: n = 15; and 18 months: n = 10. cMyBP-C(t3SD), 3 months: n = 10; 12 months: n = 13; 15 months: n = 10; and 18 months: n = 8. Data are presented as dot plots with mean ± SD. *p < 0.05 versus tWT. #p < 0.05 versus t3SD. ^p < 0.05 for 3 months versus 18 months within the same strain according to an independent Student's *t*-test. All comparisons between 3 strains were analyzed with an analysis of variance post hoc Tukey method. Multiple comparisons between all time points within the same strain were not performed.

body weight and heart weight/tibia length ratios, suggesting hypertrophy (**Figures 2D and 2E**). Meanwhile, cMyBP-C(t3SD) and cMyBP-C(tWT) mice exhibited similar lung/body, heart/body, and heart/tibia length ratios. Combination of increased lung/body weight ratio, heart/body weight ratio, worst cardiac dysfunction according to echocardiography (described in the following section), and lowest survival represented signs of HF in the hypophosphorylated cMyBP-C(t3SA) mice.

cMyBP-C(t3SD) PHOSPHORYLATED-MIMETIC AGED MICE SHOWED BETTER PRESERVATION OF DIASTOLIC AND SYSTOLIC FUNCTIONS BY ECHOCARDIOGRAPHY. Echocardiography was used to study in vivo cardiac structure and function starting at 3 months until 18 months of age (**Figures 3A to 3G**, Supplemental Figure 1, Supplemental Table 1). All mice had similar heart rates (**Figure 3B**). cMyBP-C(t3SA) hearts showed hypertrophy as seen by increased LV posterior wall thickness at diastole starting at 3 months of age.

FIGURE 4   cMyBP-C Phosphorylated Mimetic (t3SD) Preserves Myocardial Relaxation With Aging Independently of $[Ca^{2+}]_i$ Kinetics
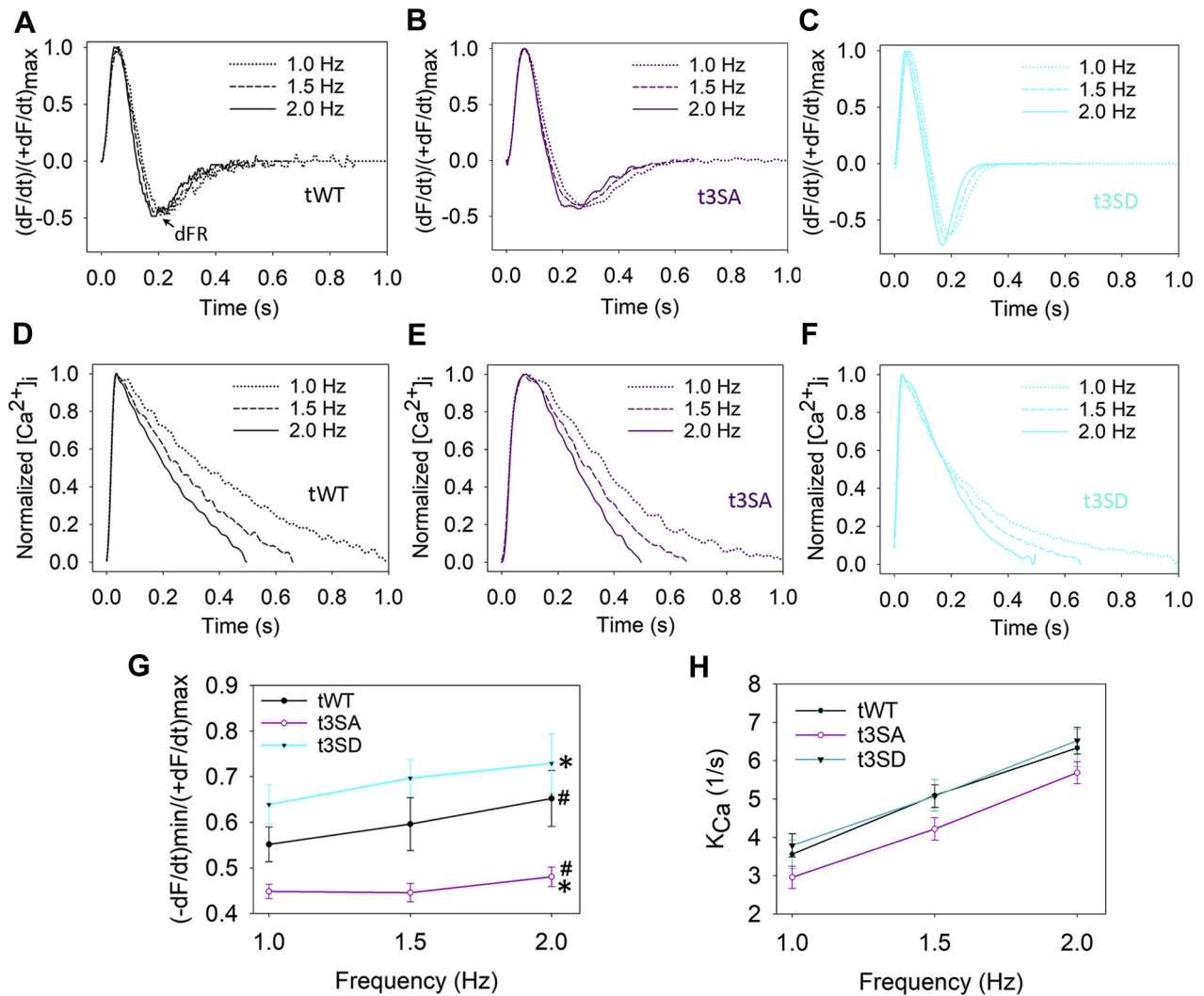
tWT: n=4 t3SA: n=4; t3SD: n=5, Error Bar=SEM; *p<0.05 vs tWT; #p<0.05 vs t3SD

Force and intracellular calcium $[Ca^{2+}]_i$ were simultaneously measured on intact papillary muscles from mouse models 12 to 15 months old with increasing pacing frequency (1.0 to 2.0 Hz). **(A to C)** cMyBP-C(t3SD) showed greater acceleration of relaxation in response to increased pacing frequency with increasing magnitude of dFR, dFR = $[(-dF/dt)_{min}/(+dF/dt)_{max}]$. **(D to F)** Normalized $[Ca^{2+}]_i$ traces show that increasing pacing frequency shortens $[Ca^{2+}]_i$ decay times in a similar manner for all models. **(G)** Increased pacing frequency causes faster relaxation in the cMyBP-C(t3SD) aged model. **(H)** Increasing pacing frequency causes similar increases in the $[Ca^{2+}]_i$ decay rate constant (k_{Ca}) in all mouse models. Repeated measure analysis of variance with intergroup comparison was used to identify significant differences in responses to increasing pacing frequency on intact papillary muscles among the 3 strains.

cMyBP-C(tWT) increased LV wall thickness at diastole with aging (**Figure 3D**, Supplemental Table 1). Meanwhile, cMyBP-C(t3SD) hearts maintained the same LV wall thickness throughout life. cMyBP-C(t3SD) hearts maintained an ejection fraction (EF) >45% (**Figure 3C**) and exhibited enhanced contractility with faster tissue Doppler of myocardial contraction velocity during systole (Sa) throughout aging (**Figures 3A and 3G**) compared with other strains. cMyBP-C(tWT) showed deterioration of EF from 61% at 3 months to 36% at 18 months. In addition, cMyBP-C(t3SD) hearts showed enhanced myocardial relaxation velocity during early diastole (e′) at 3, 12, 15, and 18 months and smallest blood flow Doppler (E) to e′ ratio (E/e′) at 12 months

(**Figures 3A, 3E, and 3F**). Meanwhile, cMyBP-C(t3SA) hearts exhibited impaired relaxation throughout aging as shown by the slowest e′ and the biggest E/e′ ratio.

Using a separate independent Student's *t*-test comparing only 2 mouse models at 18 months, cMyBP-C(t3SD) hearts exhibited lower E/e′ than cMyBP-C(tWT) hearts: the E/e′ values consisted of cMyBP-C(t3SD) 19.8 ± 1.3 (n = 8) and cMyBP-C(tWT) 29.4 ± 3.9 (n = 6); p = 0.021 (**Supplemental Figure 1**). The large differences between the models, resulting in a large ensemble variance with relatively small numbers at 18 months, likely made the ANOVA-Tukey method unable to detect differences among the 3 models despite dot plots indicating differences of E/e′ and significant differences according to the Student's *t*-test (**Figure 3F**). Thus, phosphorylation mimetic cMyBP-C(t3SD) hearts exhibited better preservation of systolic function (greater EF and Sa) and diastolic function (faster e′ and smaller E/e′) with aging. In contrast, hypophosphorylated mimetic cMyBP-C(t3SA) hearts, as previously shown (6), first present as HF with preserved EF (with predominant diastolic dysfunction, EF >50%, and evidence of pulmonary edema) and then deteriorate into HF with reduced EF (EF <30%) and diastolic dysfunction. Similar to cMyBP-C(t3SA), cMyBP-C(tWT) hearts exhibit hypertrophy, deterioration of systolic function, and deterioration of diastolic function with aging.

INTACT PAPILLARY MUSCLES FROM PHOSPHORYLATED MIMETIC AGED MICE MODEL SHOWED FASTEST RATES OF RELAXATION. We simultaneously measured force and intracellular calcium concentration $[Ca^{2+}]_i$ on intact papillary muscles from aged mice hearts to differentiate contributions of $[Ca^{2+}]_i$ handling versus cross-bridge detachment rates. For this purpose, intact papillary muscles from mice 12 to 15 months old were isolated. Increasing pacing frequency was used to mimic increasing heart rate during exercise stress. We used the peak relaxation rate $(-dF/dt)_{min}$ to peak force generation rate $(+dF/dt)_{max}$ ratio, $dFR = [(-dF/dt)_{min}/(+dF/dt)_{max}]$, to compare lusitropy of intact papillary muscles and to assess the effect of increasing pacing frequency in all 3 models. Normalization of $(-dF/dt)_{min}$ to $(+dF/dt)_{max}$ adjusted for an increasing peak rate of relaxation as a result of increasing rate of peak contraction; therefore, enhancement of relaxation beyond what is expected due to increased contractility will manifest as increasing dFR because $(-dF/dt)_{min}$ increase > $(+dF/dt)_{max}$ increase. Increased pacing frequency accelerated relaxation, which is manifested as increasing dFR in cMyBP-C(tWT) and cMyBP-C(t3SD) but not in cMyBP-C(t3SA) (**Figures 4A to 4C**).

cMyBP-C(t3SD) and cMyBP-C(tWT) consistently exhibited greater dFR, meaning enhanced relaxation (**Figure 4G**). Furthermore, cMyBP-C(t3SD) showed the highest dFR, suggesting that persistent cMyBP-C phosphorylation provided the best rates of relaxation. A single negative exponential was used to calculate the $[Ca^{2+}]_i$ decay rate constant; all models showed similar rate constant values (**Figures 4D to 4F and 4H**). Therefore, enhanced relaxation in cMyBP-C(t3SD) is attributed to cross-bridge cycling but not differences in $[Ca^{2+}]_i$ handling.
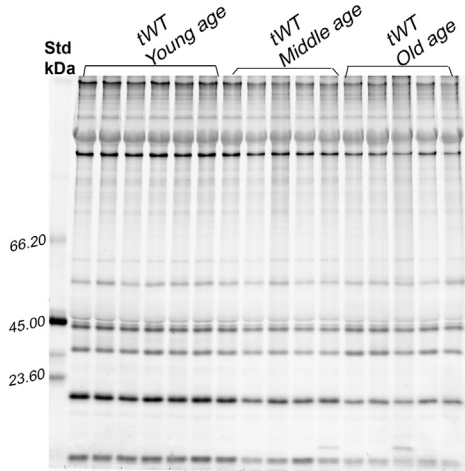
cMyBP-C PHOSPHORYLATION DECREASES WITH AGING IN THE cMyBP-C(tWT) STRAIN. Phosphorylated-protein staining showed that middle-aged (9 months) and old-age (18 to 24 months) cMyBP-C(tWT) mice exhibited reduced total cMyBP-C phosphorylation compared with the younger counterpart cMyBP-C(tWT) (2 to 6 months) (**Figures 5A to 5C**). Moreover, Western blot analyses revealed that aging significantly decreased cMyBP-C phosphorylation at S273 and S282 (**Figures 5D and 5E**) but not at S302 (**Figure 5F**). Pearson correlation analyses consisting of mice at their age according to month (2, 4 ,6, 9, 18, and 24) and site-specific phosphorylation level revealed that cMyBP-C phosphorylation at S273-P and S282-P decreased in a linear fashion with age (**Figure 6**). Thus, decreased levels of cMyBP-C phosphorylation in the aging hearts should be considered as an important contributor to aging-related cardiac dysfunction.

cMyBP-C PHOSPHORYLATION MUTATIONS ALTERED PHOSPHORYLATION OF OTHER MYOFILAMENT PROTEINS WITH AGING. At a young age, all 3 strains showed similar tropomyosin, cardiac troponin I (cTnI), regulated myosin light chain, and titin phosphorylation levels (**Supplemental Figure 2**). These findings are similar to those from our previous study (6). Moreover, we detected no differences in cTnI, regulated myosin light chain, or titin phosphorylation among the 3 strains at old age. However, both cMyBP-C(t3SA) and cMyBP-C(t3SD) strains exhibited different cardiac troponin T and tropomyosin phosphorylation levels than cMyBP-C(tWT) with aging. Unlike the other 2 strains, aging changed tropomyosin and regulated myosin light chain phosphorylation in the cMyBP-C(t3SA) model. The cMyBP-C(t3SA) model exhibited both reduced contractility (15) and impaired relaxation (6,15) at 3 months of age; therefore, these myofilament phosphorylation differences are likely caused by long-term response to inherent myofilament dysfunction.
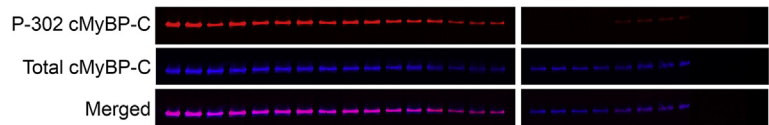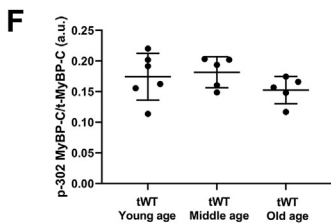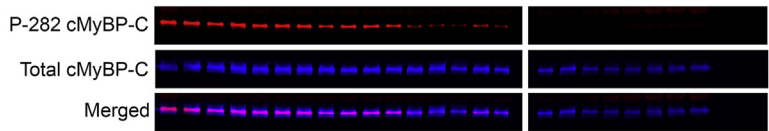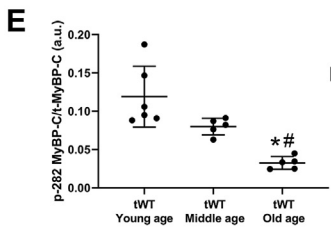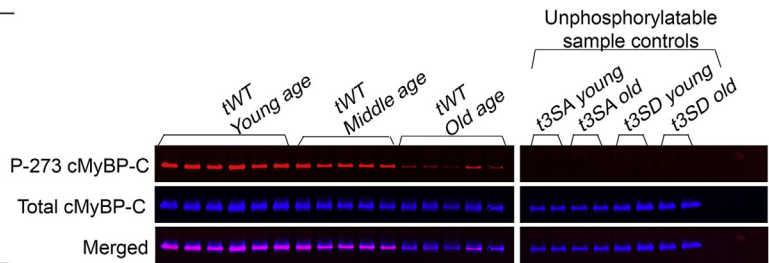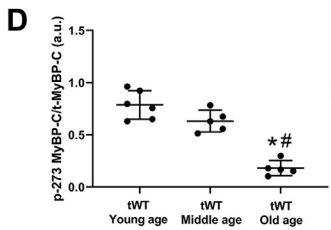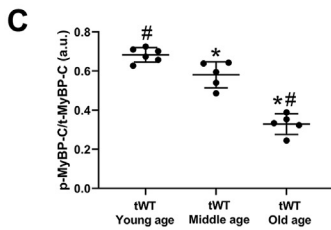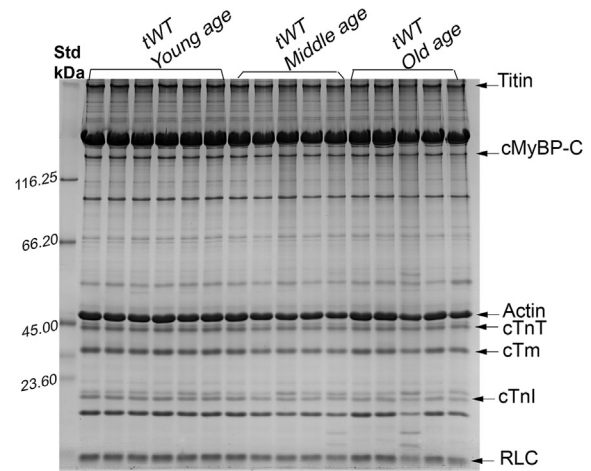
AGED MICE SHOWED SIMILAR LEVELS OF FIBROSIS. HOP levels were determined to assess

FIGURE 5 cMyBP-C Phosphorylation Decreases With Aging in cMyBP-C(tWT) Strain

*p < 0.05 vs. tWT-Young age, #p<0.05 vs. tWT-Middle age. tWT-Young age n=6, tWT-Middle age n=5, tWT-Old age n=5.
Unphosphorylatable sample controls: n=2

whether differences in tissue fibrosis in the aged mice contributed to the observed differences in diastolic function, systolic function, and hypertrophy. The HOP assay is a method that directly quantifies tissue collagen. We found no differences in the amount of HOP content between the 3 mouse models in the aged hearts or young hearts (Figure 7). Because there were no significant differences in the amount of HOP between mouse models, we could not attribute heart function and structure differences among the 3 models to differences in fibrosis. However, the cMyBP-C(t3SA) aged hearts exhibited significantly higher HOP content than their younger counterparts. This finding could explain the more severe decline in systolic and diastolic functions observed in the cMyBP-C(t3SA) model with aging.

WT MICE EXHIBITED SIMILAR DECLINE IN CARDIAC FUNCTION WITH AGING. We aged the same strain of WT (SVE-129) mice as our mouse models to serve as a control to check if the cMyBP-C$^{(-/-)}$ background unduly influenced the observed aging outcomes. The WT mice age categories were young (3.0 ± 0.01 months; n = 6) and aged (23.9 ± 0.04 months, n = 6). Aging decreased EF from 82.04 ± 2.03% to 52.62 ± 5.08% (p < 0.001); increased E/e′ from 16.54 ± 1.56 to 40.62 ± 5.33 (p = 0.001); and induced hypertrophy in which LV posterior wall thickness at diastole increased from 0.84 ± 0.08 mm to 1.22 ± 0.06 mm (p = 0.004). Thus, aging caused systolic dysfunction, diastolic dysfunction, and hypertrophy in WT mice in a fashion similar to our cMyBP-C models (Supplemental Table 2).

DISCUSSION

MAINTAINING cMyBP-C PHOSPHORYLATION MITIGATED AGE-RELATED DEVELOPMENT OF CARDIAC DYSFUNCTION.
We aged mouse models of cMyBP-C phosphorylation

mimetic cMyBP-C(t3SD), cMyBP-C phosphorylation-deficient cMyBP-C(t3SA), and wild-type cMyBP-C(tWT) to test the hypothesis that cMyBP-C phosphorylation can resist age-related development of cardiac dysfunction. Echocardiographic studies revealed that the phosphorylation mimetic cMyBP-C(t3SD) exhibited better preservation of systolic function, diastolic function, and structure with aging. Importantly, phosphorylation mimetic cMyBP-C(t3SD) mice also exhibited superior survival with aging. Conversely, control cMyBP-C(tWT) mice showed decreasing cMyBP-C phosphorylation along with deterioration of cardiac structure and function with aging. As expected with slowed contractility and impaired relaxation starting at a young age (6,15), the negative control cMyBP-C(t3SA) fared the worst. With aging and de-phosphorylation of cMyBP-C, the cMyBP-C(tWT) cardiac structure, cardiac function, and mortality drifted toward the cMyBP-C(t3SA) phenotype. This drift provided further evidence that cMyBP-C de-phosphorylation contributed to age-related development of cardiac dysfunction. Thus, better preservation of cardiac function and improved survival of cMyBP-C(t3SD) showed that maintaining cMyBP-C phosphorylation mitigated age-related development of cardiac dysfunction.

PRESERVATION OF CARDIAC FUNCTION DURING AGING WITH cMyBP-C PHOSPHORYLATION IS SUPPORTED BY EXISTING STUDIES.
Previously, a protein phosphatase-1 overexpression mouse model exhibited decreased cMyBP-C phosphorylation along with development of cardiac dysfunction with aging (20). Also, decreased norepinephrine-induced cMyBP-C phosphorylation was found in aged rat hearts (21). Older hypertensive dogs with heart failure with preserved ejection fraction (HFpEF) exhibited hypophosphorylation of cMyBP-C (22). These studies showed that aging

---

FIGURE 5 **Continued**

The cMyBP-C(tWT) age groups consist of: young, 2 to 6 months; middle age, 9 months; and old, 18 to 24 months. cMyBP-C(t3SA) and cMyBP-C(t3SD) strains, which have the known protein kinase-A sites mutated to nonphosphorylatable residues, served as negative controls. cMyBP-C(t3SA) age groups consist of: young, 6 months; and old, 23 months. cMyBP-C(t3SD) age groups consist of: young, 3 to 4 months; old, 20 and 24 months. **(A)** Pro-Q diamond staining of phosphorylated proteins on sodium dodecyl sulfate-polyacrylamide **gel** electrophoresis that were extracted from cMyBP-C(tWT) hearts. **(B)** Subsequent Coomassie staining of total protein on the same gel from **A**. **(C)** Quantification of cMyBP-C phosphorylation from Pro-Q–stained and Coomassie-stained gels showed that cMyBP-C phosphorylation decreased with age. **(D) (Left)** quantification of cMyBP-C S273 phosphorylation over total cMyBP-C from cMyBP-C(tWT) strain showed that aging decreased cMyBP-C phosphorylation at S273. **(Middle)** Western blotting detected cMyBP-C phosphorylation at S273 in the cMyBP-C(tWT) strain. **(Right)** Western blotting showed that mutations from serine to alanine (t3SA) or aspartic acid (t3SD) residues removed the proper epitope for S273 phospho-specific antibody recognition. **(E) (Left)** quantification of cMyBP-C S282 phosphorylation over the total cMyBP-C from cMyBP-C(tWT) strain showed that S282 phosphorylation decreased with aging. **(Middle)** Western blotting detected cMyBP-C phosphorylation at S282 in the cMyBP-C(tWT) strain. **(Right)** Western blotting showed that S to A or S to D mutations removed the proper epitope for S282 phospho-specific antibody recognition. **(F) (Left)** quantification of cMyBP-C S302 phosphorylation over total cMyBP-C from cMyBP-C(tWT) strain showed no significant changes at S302 with aging. **(Middle)** Western blotting detected cMyBP-C phosphorylation at S302 in the cMyBP-C(tWT) strain. **(Right)** **Western blotting** showed that S to A and S to D mutations removed the proper epitope for S302 phospho-specific antibody recognition. Comparisons between the 3 age-groups were analyzed with an analysis of variance post hoc Tukey method. Data are presented as dot plots with mean ± SD.

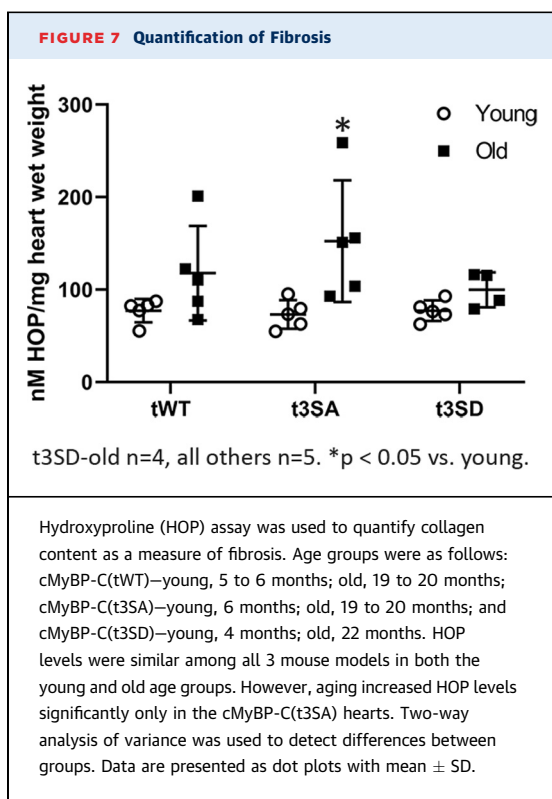**FIGURE 6   cMyBP-C Phosphorylation at S273 and S282 Decrease Linearly With Age**
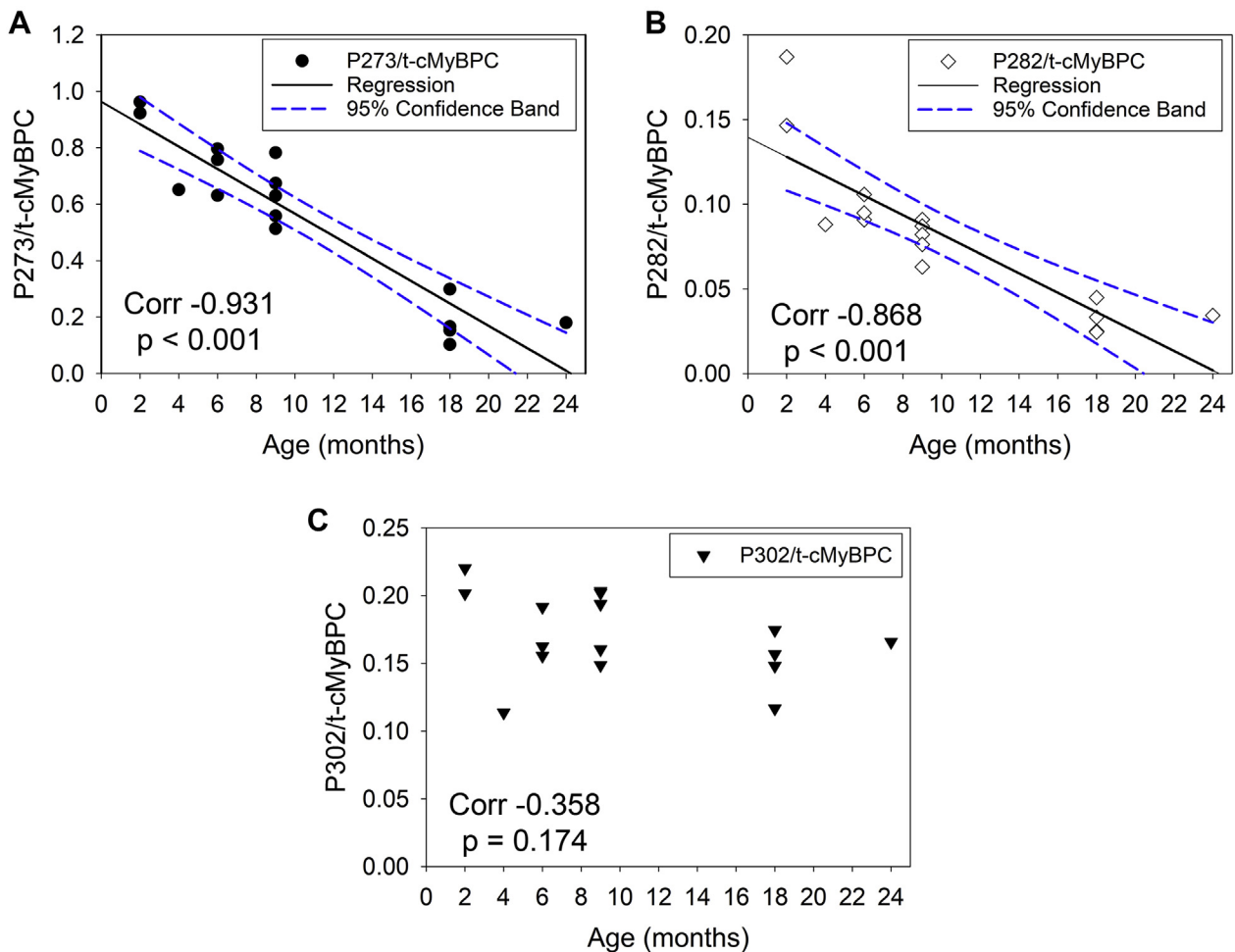
Pearson correlation analyses and linear regressions were performed on cMyBP-C site-specific phosphorylation Western blots for cMyBP-C(tWT) with n = 16 at ages 2 to 24 months. Correlation coefficient (–1 to 1) quantifies strength of correlation, in which strong is: |coefficient| >0.5; moderate is: 0.3 ≤ |coefficient| <0.5; and weak is: 0.1 ≤ |coefficient| <0.3. **(A)** Analyses showed that cMyBP-C S273 phosphorylation decreased in a strongly correlated linear fashion with increasing age. **(B)** Analyses showed that cMyBP-C S282 phosphorylation decreased in a strongly correlated linear fashion with increasing age. **(C)** cMyBP-C S302 phosphorylation did not correlate with increasing age.

correlated with decreasing cMyBP-C phosphorylation and worsening cardiac dysfunction. Exercise improved diastolic function in elderly patients with HF and reduced EF (23). Exercise also increased the phosphorylation of cMyBP-C and other contractile proteins in mice (24). Thus, it is plausible that exercise increased cMyBP-C phosphorylation to improve diastolic function. Previously, we found that phosphorylated cMyBP-C increased the force of contraction by accelerating cross-bridge cycling and, by inference, increasing the number of cross-bridges that generate force in response to dobutamine and increased pacing frequency (5). We also showed that acceleration of cross-bridge cycling by

phosphorylated cMyBP-C also resulted in enhanced relaxation (6).

In the present study, cTnI phosphorylation did not differ among the 3 mouse models; therefore, differences in function cannot be attributed to differences in cTnI phosphorylation (Supplemental Figure 2). Furthermore, similar levels of cTnI phosphorylation suggest that protein kinase-A and protein kinase-C overall activity remained similar among the 3 mouse models. We acknowledge that cardiac troponin T and tropomyosin phosphorylation levels changed in the cMyBP-C(t3SA) and cMyBP-C(t3SD) models with aging; however, we believe that these changes are compensatory mechanisms

FIGURE 7 Quantification of Fibrosis

t3SD-old n=4, all others n=5. *p < 0.05 vs. young.

Hydroxyproline (HOP) assay was used to quantify collagen content as a measure of fibrosis. Age groups were as follows: cMyBP-C(tWT)—young, 5 to 6 months; old, 19 to 20 months; cMyBP-C(t3SA)—young, 6 months; old, 19 to 20 months; and cMyBP-C(t3SD)—young, 4 months; old, 22 months. HOP levels were similar among all 3 mouse models in both the young and old age groups. However, aging increased HOP levels significantly only in the cMyBP-C(t3SA) hearts. Two-way analysis of variance was used to detect differences between groups. Data are presented as dot plots with mean ± SD.

driven by our mutations. Taken together, these results support the idea that cMyBP-C phosphorylation is a key player in the regulation and maintenance of normal systolic and diastolic functions in the elderly. Our study made a novel translation step of this concept by showing that maintaining cMyBP-C phosphorylation preserved cardiac function and improved survival with aging.

PRESERVATION OF MYOCARDIAL CONTRACTION AND RELAXATION IN AGED cMyBP-C PHOSPHORYLATION MIMETIC MICE IS LIKELY DUE TO FASTER CROSS-BRIDGE CYCLING. With echocardiography, the aged WT equivalent cMyBP-C(tWT) and the hypo-phosphorylated cMyBP-C(t3SA) model showed slower peak myocardial contraction velocities (Sa) than the phosphorylation mimetic cMyBP-C(t3SD) model (**Figure 3G**). Peak myocardial relaxation velocities (e′) were slower in the cMyBP-C(t3SA) and cMyBP-C(tWT) hearts, reflecting impaired relaxation (**Figure 3E**) (25). E/e′ ratios were higher in the cMyBP-C(t3SA) and cMyBP-C(tWT) models, suggesting compromised diastolic function (**Figure 3F**) (25). Also, cMyBP-C(t3SA) and cMyBP-C(tWT) exhibited increased posterior ventricular wall thickness with aging (**Figure 3D**), reminiscent of human LV hypertrophy with HFpEF (26,27). Similar to our findings,

echocardiographic data from humans showed that age is associated with increased LV mass (increasing wall thickness) and EF abnormalities (28,29). Meanwhile, cMyBP-C(t3SD) maintains a constant wall thickness with aging (**Figure 3D**), suggesting that cMyBP-C phosphorylation prevented remodeling. Better preservation of systolic and diastolic functions may have decreased the drive for hypertrophic response. cMyBP-C(t3SD) showed higher systolic blood pressure within the normal range, providing additional evidence of better cardiac function. Similar collagen content of aged hearts as estimated by using HOP among the 3 mouse models found that functional differences could not be attributed to fibrosis (**Figure 7**). We then performed simultaneous force and $[Ca^{2+}]_i$ on intact papillary muscles from aged mice to elucidate the underlying mechanism for better preservation of cardiac function in cMyBP-C(t3SD). Papillary muscles isolated from cMyBP-C(t3SD) aged mice showed enhanced lusitropy in response to increased pacing frequencies in the absence of differences in $[Ca^{2+}]_i$ decay rates (**Figure 4**). These results suggest that phosphorylation of cMyBP-C accelerated the rates of cross-bridge cycling, independently of $[Ca^{2+}]_i$ variations, as the underlying mechanism of an enhanced diastolic function in cMyBP-C(t3SD) aged mice.

MOUSE STRAIN BACKGROUND AND UNINTENDED GENETIC CHANGES MOST LIKELY DID NOT CAUSE THE OBSERVED DIFFERENCE. The cMyBP-C$^{(-/-)}$ background has cardiac function that is very different from WT (15). Furthermore, multiple genetic manipulation used to produce our models (6,15) could have introduced unintended gene changes. Background differences and potential unintended genetic changes could have strongly influenced the outcomes. We aged a group of WT mice in the same SVE-129 strain as our models. We found that aging WT mice developed cardiac dysfunctions (i.e., decreased EF, increased E/e′, developed hypertrophy) in a similar fashion as cMyBP-C(tWT) mouse. Thus, aging-related development of cardiac dysfunction within our models could not be attributed to cMyBP-C$^{(-/-)}$ background or unintended genetic changes.

POTENTIAL STUDY LIMITATIONS. The 3 mouse models have incomplete expression of cMyBP-C of 72% to 84% in the myofilaments (6). However, because cMyBP-C expression levels among the models are similar, the functional differences are most likely caused by the phosphorylation status. Our study did not address murine cMyBP-C phosphorylation sites outside of S273, S282, and S302

(12,30); therefore, the phosphorylation of more recently identified sites can either enhance or oppose the effects seen in this study. To address these limitations, we will develop a new knock-in mouse model with 100% expression level and better coverage of additional important phosphorylation sites.

We fully understand that many changes occur with the aging heart (31,32). In this context, cMyBP-C phosphorylation is only 1 of the contributors. Aging will decrease phosphorylation of other myofilament proteins. Furthermore, our cMyBP-C phosphorylation mimetic mutations altered phosphorylation of other myofilament proteins differently with aging. These alterations are likely to be compensatory responses to functional differences caused by our mutations. Thus, a follow-on study of mimicking isolated cMyBP-C phosphorylation with cardiac trophic adeno-associated virus expression of cMyBP-C phosphorylation mimetics after aging is needed to better define specificity of the cMyBP-C phosphorylation effect. We also understand that our results need to be confirmed in a large animal model that better resembles humans.

CONCLUSIONS

We aged mouse models to test the hypothesis that cMyBP-C phosphorylation can mitigate age-related development of cardiac dysfunction. Superior survival, better preservation of cardiac function, and preservation of structure in the cMyBP-C(t3SD) model combined to show that maintaining cMyBP-C phosphorylation mitigated age-related development of cardiac dysfunction. Intact papillary muscle experiments showed that faster cross-bridge detachment rates independent of calcium re-uptake are a contributing mechanism.

ADDRESS FOR CORRESPONDENCE: Dr. Paola C. Rosas, Department of Physiology and Biophysics, Center for Cardiovascular Research, University of Illinois, 835 South Wolcott Avenue, Chicago, Illinois 60612. E-mail: prosas@uic.edu. OR Dr. Carl W. Tong, Department of Medical Physiology, Texas A&M University, 8447 Riverside Parkway, RM 2346 MREB-2, Bryan, Texas 77807. E-mail: CTong@tamu.edu.

PERSPECTIVES

COMPETENCY IN MEDICAL KNOWLEDGE: This paper helps readers to improve or maintain medical knowledge core competency by describing the novel mechanism by which cMyBP-C phosphorylation increases cross-bridge cycling rates to improve cardiac function; consequently, this mechanism holds potential to treat age-related heart failure.

TRANSLATIONAL OUTLOOK: Our study showed that maintaining cMyBP-C phosphorylation can preserve systolic and diastolic functions, resulting in improved survival with aging. This is a novel finding. The underlying mechanism of increasing cross-bridge detachment rates can be a central method that compensates for multiple upstream causes (e.g., aging, hypertension, diabetes). Furthermore, cMyBP-C phosphorylation also holds potential to treat HFpEF by improving diastolic function. Our results place phosphorylation of cMyBP-C at the beginning of translation toward treatment. Thus, the logical next steps include developing methods to increase cMyBP-C phosphorylation in vivo and verifying our mouse model findings in a large animal model. These methods include inhibiting phosphatase that dephosphorylates cMyBP-C and by using adeno-associated virus to perform gene therapy of expressing phosphorylated cMyBP-C mimetic. The use of 3-dimensional human pluripotent stem cell–derived engineered heart tissue could be used to verify cMyBP-C phosphorylation effects on representative human cardiac tissue. Completion of these next steps will ready the cMyBP-C phosphorylation mechanism for human clinical trial. With an aging population and lack of treatment for HFpEF, this mechanism needs to be translated to a new treatment.

REFERENCES

1. Benjamin EJ, Muntner P, Alonso A, et al. Heart disease and stroke statistics—2019 update: a report from the American Heart Association. Circulation 2019;139:e56–66.

2. Heidenreich PA, Albert NM, Allen LA, et al. Forecasting the impact of heart failure in the United States: a policy statement from the American Heart Association. Circ Heart Fail 2013;6:606–19.

3. Borlaug BA, Redfield MM, Melenovsky V, et al. Longitudinal changes in left ventricular stiffness: a community-based study. Circ Heart Fail 2013;6:944–52.

4. Blecker S, Paul M, Taksler G, Ogedegbe G, Katz S. Heart failure–associated hospitalizations in the United States. J Am Coll Cardiol 2013;61:1259–67.

5. Tong CW, Wu X, Liu Y, et al. Phosphoregulation of cardiac inotropy via myosin binding protein-C during increased pacing frequency or beta1-adrenergic stimulation. Circ Heart Fail 2015;8:595–604.

6. Rosas PC, Liu Y, Abdalla MI, et al. Phosphorylation of cardiac myosin-binding protein-C is a critical mediator of diastolic function. Circ Heart Fail 2015;8:582–94.

7. Donaldson C, Palmer BM, Zile M, et al. Myosin cross-bridge dynamics in patients with

hypertension and concentric left ventricular remodeling. Circ Heart Fail 2012;5:803–11.

8. El-Armouche A, Boknik P, Eschenhagen T, et al. Molecular determinants of altered Ca2+ handling in human chronic atrial fibrillation. Circulation 2006;114:670–80.

9. Copeland O, Sadayappan S, Messer AE, Steinen GJ, van der Velden J, Marston SB. Analysis of cardiac myosin binding protein-C phosphorylation in human heart muscle. J Mol Cell Cardiol 2010;49:1003–11.

10. van Dijk SJ, Paalberends ER, Najafi A, et al. Contractile dysfunction irrespective of the mutant protein in human hypertrophic cardiomyopathy with normal systolic function. Circ Heart Fail 2012; 5:36–46.

11. Jacques AM, Copeland O, Messer AE, et al. Myosin binding protein C phosphorylation in normal, hypertrophic and failing human heart muscle. J Mol Cell Cardiol 2008;45:209–16.

12. Kooij V, Holewinski RJ, Murphy AM, Van Eyk JE. Characterization of the cardiac myosin binding protein-C phosphoproteome in healthy and failing human hearts. J Mol Cell Cardiol 2013; 60:116–20.

13. Harris SP, Lyons RG, Bezold KL. In the thick of it: HCM-causing mutations in myosin binding proteins of the thick filament. Circ Res 2011;108: 751–64.

14. Harris SP, Bartley CR, Hacker TA, et al. Hypertrophic cardiomyopathy in cardiac myosin binding protein-C knockout mice. Circ Res 2002; 90:594–601.

15. Tong CW, Stelzer JE, Greaser ML, Powers PA, Moss RL. Acceleration of cross-bridge kinetics by protein kinase A phosphorylation of cardiac myosin binding protein C modulates cardiac function. Circ Res 2008;103: 974–82.

16. Tong CW, Gaffin RD, Zawieja DC, Muthuchamy M. Roles of phosphorylation of myosin binding protein-C and troponin I in mouse cardiac muscle twitch dynamics. J Physiol 2004; 558:927–41.

17. Solaro RJ, Pang DC, Briggs FN. The purification of cardiac myofibrils with Triton X-100. Biochim Biophys Acta 1971;245:259–62.

18. Pena JR, Szkudlarek AC, Warren CM, et al. Neonatal gene transfer of Serca2a delays onset of hypertrophic remodeling and improves function in familial hypertrophic cardiomyopathy. J Mol Cell Cardiol 2010;49:993–1002.

19. Whelton PK, Carey RM, Aronow WS, et al. 2017 ACC/AHA/AAPA/ABC/ACPM/AGS/APhA/ASH/ASPC/ NMA/PCNA guideline for the prevention, detection, evaluation, and management of high blood pressure in adults: a report of the American College of Cardiology/American Heart Association Task Force on Clinical Practice Guidelines. J Am Coll Cardiol 2018;71:e127–248.

20. Florea S, Anjak A, Cai WF, et al. Constitutive phosphorylation of inhibitor-1 at Ser67 and Thr75 depresses calcium cycling in cardiomyocytes and leads to remodeling upon aging. Basic Res Cardiol 2012;107:279.

21. Sakai M, Danziger RS, Staddon JM, Lakatta EG, Hansford RG. Decrease with senescence in the norepinephrine-induced phosphorylation of myofilament proteins in isolated rat cardiac myocytes. J Mol Cell Cardiol 1989;21:1327–36.

22. Hamdani N, Bishu KG, von Frieling-Salewsky M, Redfield MM, Linke WA. Deranged myofilament phosphorylation and function in experimental heart failure with preserved ejection fraction. Cardiovasc Res 2013;97:464–71.

23. Sandri M, Kozarez I, Adams V, et al. Age-related effects of exercise training on diastolic function in heart failure with reduced ejection fraction: the Leipzig Exercise Intervention in Chronic Heart Failure and Aging (LEICA) Diastolic Dysfunction Study. Eur Heart J 2012;33:1758–68.

24. Davis RT 3rd, Simon JN, Utter M, et al. Knockout of p21-activated kinase-1 attenuates exercise-induced cardiac remodelling through altered calcineurin signalling. Cardiovasc Res 2015;108:335–47.

25. Nagueh SF, Smiseth OA, Appleton CP, et al. Recommendations for the evaluation of left ventricular diastolic function by echocardiography: an update from the American Society of Echocardiography and the European Association of Cardiovascular Imaging. J Am Soc Echocardiogr 2016;29:277–314.

26. Zile MR, Gottdiener JS, Hetzel SJ, et al. Prevalence and significance of alterations in cardiac structure and function in patients with heart failure and a preserved ejection fraction. Circulation 2011;124:2491–501.

27. Mohammed SF, Hussain S, Mirzoyev SA, Edwards WD, Maleszewski JJ, Redfield MM. Coronary microvascular rarefaction and myocardial fibrosis in heart failure with preserved ejection fraction. Circulation 2015;131:550–9.

28. Gardin JM, Siscovick D, Anton-Culver H, et al. Sex, age, and disease affect echocardiographic left ventricular mass and systolic function in the free-living elderly. The Cardiovascular Health Study. Circulation 1995;91:1739–48.

29. Lakatta EG, Levy D. Arterial and cardiac aging: major shareholders in cardiovascular disease enterprises: part II: the aging heart in health: links to heart disease. Circulation 2003;107: 346–54.

30. Jia W, Shaffer JF, Harris SP, Leary JA. Identification of novel protein kinase A phosphorylation sites in the M-domain of human and murine cardiac myosin binding protein-C using mass spectrometry analysis. J Proteome Res 2010;9:1843–53.

31. Lakatta EG. Arterial and cardiac aging: major shareholders in cardiovascular disease enterprises: part III: cellular and molecular clues to heart and arterial aging. Circulation 2003;107:490–7.

32. Paneni F, Diaz Canestro C, Libby P, Luscher TF, Camici GG. The aging cardiovascular system: understanding it at the cellular and clinical levels. J Am Coll Cardiol 2017;69:1952–67.

KEY WORDS aging, cardiac myosin binding protein-C, dyastolic dysfunction, heart failure, phosphorylation

---

APPENDIX For supplemental tables and figures, please see the online version of this paper.